FCC-ee Physics, Experiments, and Detectors

– – *

A. Blondel[1], C. Grojean[2,3], P. Janot[4] and M. McCullough[4] (editors);

P. Azzi[5], P. Azzurri[6], N. Bacchetta[5], C. Bernet[7], F. Blekman[19], M. Boscolo[8], M. Dam[9], D. d'Enterria[4], J. Ellis[10], A. Freitas[11], B. Hegner[4], S. Heinemeyer[xx], C. Helsens[4], J. Kamenik[12], H. Khanpour[20], S. Khatibi[20], M. Khatiri[20], M. Klute[13], N. van der Kolk[4], E. Leogrande[4], C. Leonidopoulos[14], S. Monteil[15], E. Perez[4], K. Peters[2], F. Piccinini[16], M. Pierini[4], C. Rogan[17], G. Rolandi[4], R. Tenchini[6], F. Simon[21], P. Skands[18], K. Skovpen[19], G. Voutsinas[4], J. Wenninger[4].

[1] University of Geneva, CH-1205 Geneva, Switzerland
[2] DESY, Notkestraße 85, D-22607 Hamburg, Germany
[3] Humboldt Universität zu Berlin, Newtonstraße 15, D-12489 Berlin, Germany
[4] CERN, CH-1211 Geneva 23, Switzerland
[5] INFN, Sezione di Padova, Via Marzolo 8, 35131 Padova, Italy
[6] INFN, Sezione di Pisa, Largo Bruno Pontecorvo, 3, 56127 Pisa, Italy
[7] Institut de Physique Nucléaire de Lyon, CNRS/IN2P3, 69622 Villeurbanne, France
[8] INFN, Laboratori Nazionali di Frascati, Via Enrico Fermi 40, 00044 Frascati, Italy
[9] Niels Bohr Institute, University of Copenhagen, Blegdamsvej 17, 2100 Copenhagen, Denmark
[10] King's College London, Strand, London WC2R 2LS, UK,
[11] University of Pittsburgh, Department of Physics and Astronomy, 3941 O'Hara St, Pittsburgh, PA 15260, USA
[12] Josef Stefan Institute, Theory Department, Jamova cesta 39, 1000 Ljubljana, Slovenia
[13] Massachusetts Institute of Technology, 77 Massachusetts Ave, Cambridge, MA 02139, USA
[14] University of Edinburgh, , Department of Physics and Astronomy, Old College, South Bridge, Edinburgh EH8 9YL, UK
[15] Laboratoire de Physique de Clermont, CNRS/IN2P3, 63178 Aubière Cedex, France
[16] Università di Pavia and INFN, Sezione di Pavia, Via A. Bassi, 6, 27100 Pavia, Italy
[17] Harvard University, Cambridge, MA 02138, USA
[18] Monash University, School of Physics and Astronomy, Clayton VIC 3800, Australia
[19] Interuniversity Institute for High Energies, Vrije Universiteit Brussel, Pleinlaan 2, 1050 Brussels, Belgium
[20] Institute for Research in Fundamental Sciences (IPM), P.O.Box 19395-5531, Tehran, Iran

[21] Max-Planck-Institut für Physik (Werner-Heisenberg-Institut)
Föhringer Ring 6, 80805 München, Germany

Abstract
This document is a writeup for the review of the FCC-ee physics, experiments, and detectors that took place during the FCC week in Berlin (29 May-2 June 2017). It will serve as input to the FCC Conceptual Design Report, to be made public at the end of 2018.

Contents

Chapter 1

Introduction

1 Overview

This is the first chapter of our history. The original physics considerations of a 100km e^+e^- storage ring collider were descibed in [1].

2 Operation model

This is some other text here.

Chapter 2

Electroweak physics at the Z pole

1 Introduction

To be completed by **Roberto** *by* **9th January**. *Will be done after all other sections are completed, to avoid repetitions.*

A compilation of all measurements performed at the Z pole by LEP and SLC can be found in Ref. [2].

List the physics observables accessible at the Z pole (Z lineshape, Z partial widths, Z invisible width and number of neutrinos, asymmetries, $\alpha_{\rm QED}$, $\alpha_{\rm S}$, and the current experimental and theoretical accuracies.

Introduce the need for beam energy and luminosity measurement, and recall the ultimate precision at LEP.

Give the outline of the chapter, as well as the objectives (requirements on luminosity measurement, beam energy measurement, detector designs, theory calculations, experimental uncertainties ...)

2 Luminosity measurement

The typical reference process for the luminosity determination at e^+e^- colliders is Bhabha scattering. In particular, at LEP, small angle Bhabha scattering, with electron/positron scattering angles of the order of few degrees, has been used, because, in such kinematical conditions, the contributions to the scattering amplitude due Z-boson exchange diagrams are suppressed with respect to the photon exchange diagrams. As a consequence, small angle Bhabha scattering around the Z peak is essentially a pure QED process, very weakly dependent on Z physics and characterized by a very large cross sections (of the order of 10-100 nb, for typical event selections).

In principle Bhabha scattering cross section can be calculated by means of perturbative QED with arbitrary precision; the perturbative calculations of higher order photonic corrections used at LEP relied on the exact knowledge of terms of $\mathcal{O}(\alpha L, \alpha, \alpha^2 L^2)$ at the level of fully exclusive event generation, provided by the Monte Carlo generator BHLUMI [**?**, **?**, **?**]. Additional sources of radiative corrections at one and two-loops are the photon vacuum polarization and the emission of virtual and real pairs, mainly electrons and muons, respectively. While the latter can be calculated perturbatively in QED, the former can not, because of the presence of the hadronic nonperturbative contributions. It is usually calculated by means of dispersion relation techniques. At the end of LEP data analysis, the total theoretical uncertainty on the Bhabha scattering cross sections has been estimated to be 0.061% [**?**, **?**]. This number was decreased to 0.054% by including the effect of light-pair emission [**?**, **?**]. Among the different sources of uncertainty, the two dominant contributions were estimated to be the vacuum polarization [**?**, **?**, **?**] (0.04%) and the $\mathcal{O}(\alpha^2 L)$ terms (0.027%), missing (or partially taken into account) in the Next-to-Leading-Order (NLO) calculations matched to Leading Logarithmic higher orders used for those studies. Concerning the latter, during the last decade several improved perturbative calcu-

lations have been carried out with Next-to-Next-to-Leading-Order (NNLO) accuracy: NNLO photonic corrections [**?**, **?**, **?**], NNLO leptonic-loop corrections [**?**, **?**, **?**, **?**], heavy fermion and hadronic loops contributing to NNLO accuracy [**?**, **?**, **?**, **?**, **?**], NLO soft plus virtual corrections to single hard bremsstrahlung [**?**]. Recent developments in perturbative higher order calculations for Bhabha scattering and their implementation in Monte Carlo generators have been reported in Ref. [**?**].

Already at present all perturbative ingredients for a theoretical uncertainty in small angle Bhabha scattering at the 0.01% level are available, even if the recipe for building a so called NNLOPS event generator, i.e. NNLO accuracy plus Leading Logarithmic higher order corrections, is not yet available. The bottleneck towards high precision is given by the hadronic contribution to the vacuum polarization, $\Delta\alpha_h(M_Z^2)$. In fact this contribution cannot be calculated perturbatively but we have to rely on a dispersion relation which uses the experimental data of the $e^+e^- \to$ hadrons cross section, measured at the low energy e^+e^- flavour factories. Thanks to the measurements performed during last years, we have now new parameterizations [**?**, **?**, **?**], which lead to $\Delta\alpha_h(M_Z^2)$ estimates with reduced errors by about a factor of five with respect to the parameterizations of Refs. [**?**,**?**]. By using these parameterizations, the uncertainty affecting small angle Bhabha scattering around the Z resonance can be estimated to be of the order of 0.02% [**?**] [1]. Future available data from high luminosity flavour factories, such as BEPC and SuperKEKB, could allow an improved precision on $\Delta\alpha_h(M_Z^2)$ of about a factor of two.

Experimentally, low-angle Bhabha scattering is measured by detecting two back-to-back electrons on both sides of the apparatus, in a fiducial acceptance corresponding to two annuli defined by radii R_{min} and R_{max}, equivalent to the angular region between the polar angles θ_{min} and θ_{max}, corresponding to the integrated Rutherford cross section

$$\sigma_{bh}^{th} \sim \frac{16\pi\alpha^2}{s}\left(\frac{1}{\theta_{min}^2} - \frac{1}{\theta_{max}^2}\right) .$$

To computed the expected cross section precisely, the fiducial acceptance need to be known precisely, for a typical value of R_{min} around 50 mm and an accuracy in detector position of 10 micron (similar to the accuracy reached at LEP), the systematic error on the luminosity is $\Delta L/L \simeq 2\Delta R_{min}/R_{min} \simeq 4 \cdot 10^{-4}$. Therefore to match the expected improvement in theoretical accuracy for the Bhabha scattering (0.01%) an accuracy in detector position of ≈ 2 microns should be reached, which looks feasible already with present technology. It must be kept in mind that nn appropriate choice of the event selection cuts can largely remove the dependence of the luminosity on the relative position between the beams interaction point and the detector, as proposed in [**?**]. If two different fiducial regions are defined for the two luminosity detectors positioned at the left and right sides with respect to the interaction point, the luminosity measurement can be made independent of transverse misalignments. The dependence on longitudinal misalignments is also largely canceled if the definition of loose and tight is changed from one side to the other side randomly on an event by event basis. In conclusion a precision on the determination of luminosity from low-angle Bhabha scattering of $\approx 0.01\%$ can be expected, both from the theoretical and experimental point of view.

In principle, an alternative process, which could allow to overcome the limitation in the precision luminosity determination, is the photon pair production $e^+e^- \to \gamma\gamma$. In fact, for this process, the vacuum polarization correction starts to contribute at NNLO level. Moreover, at

[1] The results have been obtained by means of the Monte Carlo event generator BabaYaga@NLO [**?**, **?**, **?**, **?**].

tree level, photon-pair production is free of Z-exchange diagrams. At present, the theoretical level of knowledge for this process is NLOPS [**?**], i.e. NLO matched to Leading Logarithmic higher order corrections, which corresponds to a theoretical uncertainty at the 0.1% level. The shortcoming of photon pair production with respect to Bhabha scattering is the lower cross section, in the range of 10-100 pb [**?**] for large angle event selections, which would require an integrated luminosity of $1.4ab^{-1}$ to reach correspond a statistical error of the order of 0.01%, similar to the one expected for low-angle Bhabha scattering. In addition, photon reconstruction efficiency and rejection against Bhabha scattering events should be carefully analyzed, in order to consider photon pair production as a relevant channel for precision luminosity determination.

3 The Z lineshape

The scan of the Z resonance provides two parameters playing a key role for the understanding of electroweak interactions: the mass of the Z vector boson and its width. As can be seen from Fig. 2.1 the Z lineshape is considerably distorted by radiation of photons by the electron and positron beams: the production cross section at the peak is strongly reduced and the resonance shape becomes asymmetric, as a result of the shift in effective centre-of-mass energy. The extraction of electroweak parameters from the lineshape requires these ISR QED effects (together with FSR and their interference) to be precisely calculated and kept under control at required precision. It is convenient to define a *radiator function* ($H(s,s')$), which incorporates all ISR corrections, and a *reduced cross section* ($\hat{\sigma}_{f\bar{f}}(s')$) that are convolved in order to compute the visible cross section

$$\sigma_{f\bar{f}}(s) = \int_{4m_f^2}^{s} ds' H(s,s') \hat{\sigma}_{f\bar{f}}(s') \; . \tag{2.1}$$

for all centre-of-mass points included in the energy scan. For LEP data analysis, the radiator function has been computed up to the leading $\mathcal{O}(\alpha^3)$ order. The impact of the uncertainty on ISR corrections to the Z mass and width was computed by comparing two different calculations based either on additive (TOPAZ0) or factorized (ZFITTER) corrections. The precision was found to be of the order of 10^{-5} leading to an uncertainty on the Z mass and width of 100 KeV, which was negligible at LEP, but needs to be improved for FCC-ee with higher order calculations.

The $\hat{\sigma}$ reduced cross section, extracted after ISR de-convolution, is composed by three terms

$$\hat{\sigma}_{f\bar{f}}(s) = \sigma_{f\bar{f}}^{peak} \cdot \frac{s\Gamma_Z^2}{\left(s - \mathbf{m}_Z^2\right)^2 + \left(\frac{s\Gamma_Z}{\mathbf{m}_Z}\right)^2} \; + \text{“}(\gamma - Z)\text{”} + \text{“}|\gamma|^2\text{”} \tag{2.2}$$

corresponding to the relativistic Breit-Wigner distribution, to the photon exchange and to the non-factorisable interference term, respectively. While the photon exchange contribution does not depend on m_Z, Γ_Z and therefore poses no problem, the $\gamma - Z$ interference component requires either model dependent assumptions (i.e. assuming the Standard Model form and parameters) or a direct measurement of the cross section off the resonance. The model independent approach follows the so-called S-matrix parametrization [**?**], where the interference term corresponds to a dimensionless parameter denoted J_{had}^{tot}, whose uncertainty corresponds to a m_Z uncertainty of $\frac{\partial m_Z}{\partial J_{had}^{tot}} = -1.6 \text{ MeV}/0.1$.

At LEP1 the nominal lineshape result was obtained with the model dependent parametrization, because LEP-only data were not sufficient to provide a result with equivalent precision in the S-matrix approach. However, data collected at Tristan at the centre-of-mass energy of about 60 GeV [**?**], corresponding to an integrated luminosity of 300 pb^{-1} provided a measurement of J^{tot}_{had} with a precision of 0.1, sufficient for a model-independent lineshape-parameters measurement. At FCC-ee a sample of 100 fb^{-1} collected at the centre-of-mass energy of 60 GeV would allow J^{tot}_{had} to be measured with a precision corresponding to an uncertainty on m_Z of 100 keV. Alternatively data collected at higher centre-of-mass energy (i.e. above the Z resonance) could be used to provide a measurement of J^{tot}_{had} of equivalent precision, as shown by the model-independent determination of the Z-mass using LEP2 data [**?**]. The latter approach is conceptually equivalent, as no Z' resonance has been found up to a few TeV.

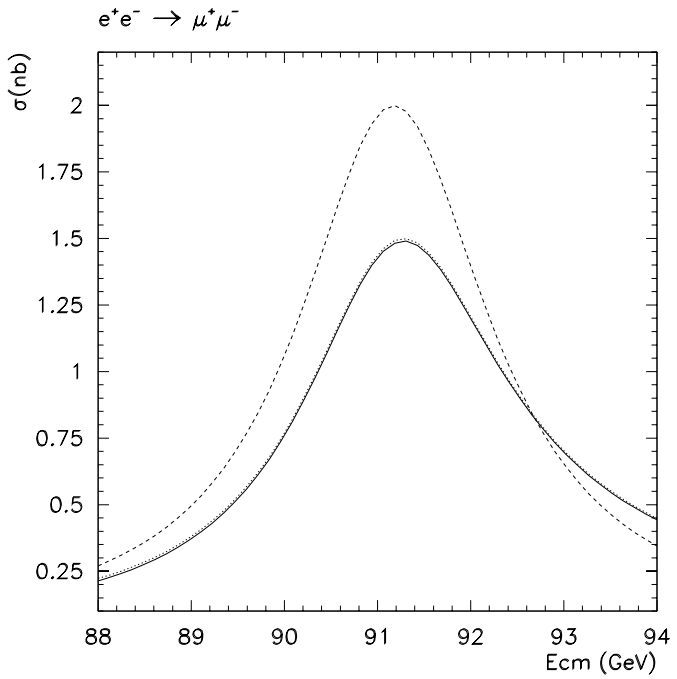

Fig. 2.1: Effect of QED initial state radiative corrections on the muon-pair production cross section near the Z pole. Cross section without initial state radiation (dashed line), $\mathcal{O}(\alpha)$ exponentiated initial state radiation (dotted line), $\mathcal{O}(\alpha^2)$ exponentiated initial state radiation (solid line).

The uncertainty on the m_Z, Γ_Z lineshape parameters is dominated by the knowledge of the centre-of-mass energy at the off-resonance points. Optimization studies performed at LEP have shown that the maximal sensitivity is obtained by collecting data at points approximately

± 2 GeV off-peak (E_{-2}, E_{+2}). The uncertainty on m_Z and Γ_Z is given approximately by

$$\Delta m_Z \approx 0.5\Delta(\mathrm{E}_{-2} + \mathrm{E}_{+2}) \tag{2.3}$$

$$\Delta\Gamma_Z \approx \frac{\Gamma_Z}{(\mathrm{E}_{-2} - \mathrm{E}_{+2})}\Delta(\mathrm{E}_{+2} - \mathrm{E}_{-2}) = 0.71\Delta(\mathrm{E}_{+2} - \mathrm{E}_{-2}) \tag{2.4}$$

i.e. the uncertainty on the Z mass (Z width) is given by the correlated (anti-correlated) uncertainty on the centre-of-mass energy at the two off peak points. As described elsewhere in this report, the beam energy is determined with extremely high precision with the technique of resonant depolarization. At LEP the width of the depolarizing resonance was as small as $\approx$ 100 keV, however the beam energy was known with a precision one-order of magnitude worse, because the energy calibration was performed in a few dedicated runs and the related information transported to the events taken during the lineshape scan. At FCC-ee the calibration is foreseen to take place continuously with dedicated non-colliding bunches: as shown in Chapter **??** $\approx$ 100 keV is a realistic goal for the knowledge of the centre-of-mass energy and corresponding uncertainty on m_Z and Γ_Z.

The beam energy spread (ϵ_{CMS}) is also affecting the lineshape because it changes the measured cross section by

$$\delta\sigma \simeq -0.5\frac{d^2\sigma}{dE^2}\epsilon^2_{CMS}\,. \tag{2.5}$$

causing a reduction of the visible cross section at peak and an increase of the cross section at the E_{-2}, E_{+2} points (the effects with the LEP optics were of the order of permil). The net effect on the mass measurement is null, however a correction for the width is required. The corresponding systematic uncertainty was negligible at LEP; as the energy spread goes as $\approx \frac{1}{\sqrt{\rho}}$, where ρ is the radius of the accelerator, and its precision will be controlled in a better way by the machine optics (Chapter **??**) the impact of the energy spread on the Γ_Z measurement is expected to be negligible at FCC-ee as well.

As will be described in next Section, the cross section are measured separately for the Z decay to hadrons and to the three lepton species. The reduced cross sections are then extracted from the data by applying the formalism previously described and the lineshape parameters can be determined in a global fit to the data. In the global fit the decays into charged lepton pairs are incorporated either by introducing in the reduced cross sections the three leptonic partial widths (Γ_e, Γ_μ and Γ_τ) or by assuming lepton universality: in this case a common leptonic width, Γ_ℓ, is determined. In the latter case four parameters are needed to describe the centre-of-mass dependence of the hadronic and leptonic cross sections: the Z mass (m_Z), the Z width (Γ_Z), the ratio of hadronic to leptonic partial width $R_\ell = \Gamma_h/\Gamma_\ell$ and the hadronic peak cross section σ^0_h. The R_ℓ and σ^0_h parameters are discussed in next Sections. Table 2.1 gives the dominating uncertainties on the four parameters and the expected precision at FCC-ee.

4 Measurement of the normalized Z partial widths

At lepton colliders decays of Z bosons to quarks and charged leptons are can be identified with high efficiency and separated from each other and from the small background even with simple criteria, as can be seen from Fig. 2.2 where only charge multiplicity and charged-track momenta are used.

Table 2.1: Dominating sources of systematic uncertainties and expected precision on lineshape parameters from a four parameter fit assuming lepton universality.

Parameter	Dominating source	expected uncertainty
m_Z	beam energy	100 keV
Γ_Z	beam energy	100 keV
σ^0_{had}	luminosity	xx nb
R_ℓ	lepton statistics	5×10^{-5}

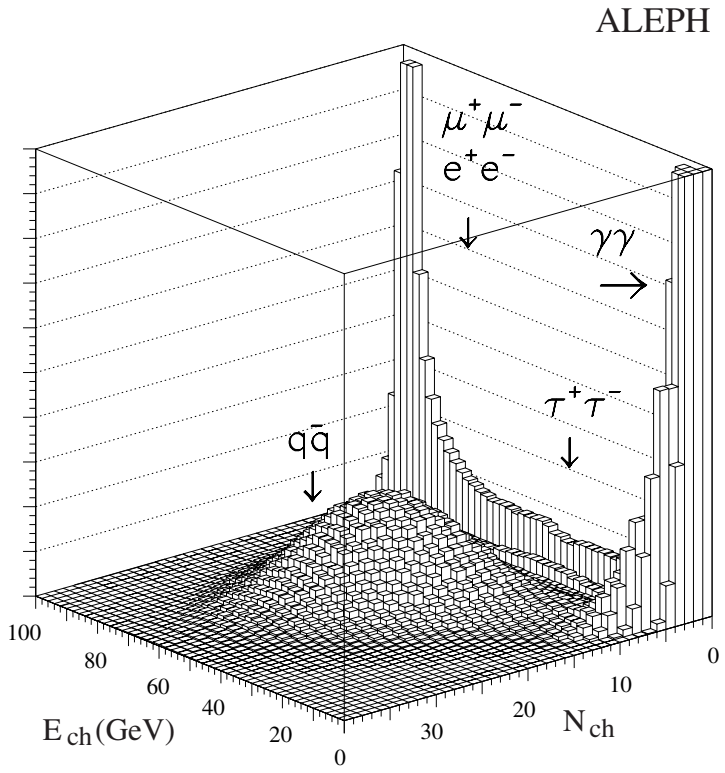

Fig. 2.2: The sum of charged track momenta versus the track multiplicity, for various final states at centre-of-mass energies around the Z peak.

At LEP a simple hadronic selection based on charged track multiplicity and visible energy reached efficiencies higher than 97% in a phase space defined as $\sqrt{\frac{s'}{s}} > 0.10$, while slightly more complex selections based on calorimeters were more than 99% efficient (here s' represents the reduced centre-of-mass energy after ISR). The inefficiency is related to events with most energy lost in the beam pipe region and can be measured from data by rotating real events. Similarly, the small contamination from non resonant two-photon events (indicated as $\gamma\gamma$ in Fig. 2.2) can be estimated from data by counting events with small visible energy as a function

of the beam energy (varied during the energy scan), because the non-resonant background is essentially energy independent. Contamination from leptons is relevant only for $\tau^+\tau^-$ events and was kept below 0.5% at LEP. Dominant systematic uncertainties in the selection were due to hadronisation modeling for a charged track selection (typically $\approx 0.05\%$) and knowledge of the detector response for a calorimeter-based selection (typically $\approx 0.10\%$). Both uncertainty can be potentially further reduced at FCC-ee with detailed studies based on data, thanks to the huge statistics.

The selection efficiency of muon pairs in appropriate fiducial regions can be made very high, as shown at LEP where the $\mu^+\mu^-$ selection efficiency was much higher than 99.9% as measured with data using tag-and-probe techniques. The fiducial region can be defined based on the scattering angle in the effective centre-of-mass system, that is

$$\cos\theta^* = \frac{\cos[\frac{1}{2}(\theta_{\ell^-} - \theta_{\ell^+} + \pi]}{\cos[\frac{1}{2}(\theta_{\ell^-} + \theta_{\ell^+} + \pi]} \tag{2.6}$$

where θ_{ℓ^-} and θ_{ℓ^+} are the scattering angles of the lepton and anti-lepton, respectively, and on the lepton collinearity, covering typically 85% of the phase space with simple cuts. Dominant systematic uncertainty are related to the knowledge of the acceptance boundaries ($\approx 0.05\%$ at LEP) and to calorimeter energy resolution in the detection of radiative $\mu^+\mu^-\gamma$ events ($\approx 0.05\%$ at LEP). Tau-pair selection is based on low particle multiplicity, narrow jets and the presence of undetected neutrinos. The latter signature can be exploited, e.g., by requiring events with large missing mass. Typical selection efficiencies for $\tau^+\tau^-$ events at LEP were higher than 80% in fiducial regions defined with simple cuts, similar to the muon pair case. For taus systematic uncertainties are dominated by contamination of other Z decays (mostly Bhabha and two-photon events), which can however be monitored with data. At LEP systematic uncertainties at the permil level were obtained. The e^+e^- final state (Bhabha scattering) requires a more complex treatment because of the presence of t-channel production, which can be suppressed by a cut on $\cos\theta^*$. The t-channel subtraction is indeed the dominant source of uncertainty for this channel ($\approx 0.10\%$ at LEP), followed by $\tau^+\tau^-$ background and knowledge of the fiducial acceptance. Improved Monte Carlo calculations, as described in Section 2 have the potential of reducing considerably this uncertainty, compared to LEP times.

In the Z lineshape fit discussed in Section 3 generic hadronic decay selections are treated together with selections of Z decays to individual lepton species and conveniently normalized to cancel the luminosity dependence, giving the ratio of hadronic to leptonic partial width $R_\ell = \sigma_{had}/\sigma_\ell = \Gamma_h/\Gamma_\ell$, where ℓ is a generic charged lepton if lepton universality is imposed. Alternatively R_e, R_μ, R_τ are obtained. At LEP the uncertainty on R_ℓ measurements was dominated by the statistics of leptonic events and therefore a combination of the three lepton species (i.e. assuming universality) provided the best result; at FCC-ee the statistical uncertainty will become neglegible, therefore the best result is expected to come from the muon channel (i.e. from a measurement of R_μ). A measurement of R_μ with a relative precision of 5×10^{-5} is in reach if the systematics related to acceptance are reduced by a factor of five with respect to LEP. This can be achieved by making measurements independent from the beam spot position and other misalignment effects, for example alternating loose and tight fiducial cuts (similarly to what is done for the luminosity measurement) and by using the high statistics to monitor detector boundaries and efficiencies (tracking uncertainties at LEP were typically of the order of 10^{-4}). In addition the description of ISR and FSR effects ($\mu^+\mu^-\gamma$ events) should be kept at the same level of control. It should be noted that the measurement will take advantage of

the increased precision on the beam energy, because $R_\ell = \sigma_{had}/\sigma_\ell$ is strictly a ration of cross sections at peak and a beam uncertainty of 100 KeV corresponds to a systematic uncertainty of 3×10^{-5}. Another uncertainty, which should be reduced, is the theoretical uncertainty on higher orders, computed at LEP by comparing ZFITTER and TOPAZ0 and corresponding to 2×10^{-4}. In this report a precision of 5×10^{-5} is considered the ultimate precision for R_μ, while for R_τ the need for controlling the e^+e^- and two-photon background suggests a precision goal of 10^{-4}. By taking into account the expected improvements in Monte Carlo simulations used for t-channel substraction a precision of 3×10^{-4} is considered for the $R_{\rm e}$ measurement.

An efficient selection of Z decays to individual quark flavours is possible only when quark's hadronization products can be efficiently tagged. This is possible for b quarks and, with lower performance, for c quarks. The use of lifetime-based b-quark tagging has been pioneered at LEP, leading to a precise measurement of $R_{\rm b}$ (with relative precision $\approx 0.3\%$). The presence of two same-flavour quarks in $\mathrm{Z} \to \mathrm{b\bar{b}}$ decays allows the measurement of b tagging efficiency (ϵ_b) directly from data by counting single (N_1^t) and double (N_2^t) tag events by using the relationships

$$N_1^t = 2\,N_{had}\,\left[R_{\rm b}\epsilon_b + R_{\rm c}\epsilon_c + (1 - R_{\rm b} - R_{\rm c})\epsilon_{uds}\right]\,, \tag{2.7}$$

$$N_2^t = N_{had}\,\left[R_{\rm b}\epsilon_b^2(1+\rho_b) + R_{\rm c}\epsilon_c^2 + (1 - R_{\rm b} - R_{\rm b})\epsilon_{uds}^2\right]\,, \tag{2.8}$$

where ϵ_c and ϵ_{uds} represents the tagging efficiency for c and light quarks, respectively. The ρ_b parameter represents the correlation between the two tags in the same event and it is the most difficult source of systematic uncertainty to be treated (the corresponding uncertainty was $\approx 0.1\%$ at LEP). Sources of correlations are essentially of three kinds: geometrical (e.g. if one b jet is close the the beam pipe, the other tends to be close, too), reconstruction-related (e.g. the same primary vertex used to compute the b-tagging significance for both tags) and related to physics (e.g. momentum correlations between the two b hadrons). The key to control tag correlations is the availability of taggers with high performance (both from the point of view of detector and software techniques): as an example high tagging efficiency, independent from the b hadron momentum, makes momentum correlations irrelevant. From the pioneering times of LEP, b-taggers have increased their efficiency by a factor three at the same c and light quark contamination level, in the much harsher conditions of LHC. In addition other sources of systematics uncertainties, e.g. related to gluon splitting and to the knowlgedge of ϵ_c, can be studied in details using data already at LHC. Here we consider a factor 3 reduction of the systematic uncertainties on tag correlations largely feasible with modern tracking detectors and taggers, leading to a target precision for $R_{\rm b}$ at FCC-ee of $\approx 0.03\%$.

A pure selection of charm jets is more challenging, however already in the nineties the SLD experiment at SLAC was able to select $\mathrm{Z} \to \mathrm{c\bar{c}}$ decays with a purity of 67% albeit with low efficiency (14%, which would be clearly sufficient at FCC-ee given the large statistics). Charm jets are characterized by the shorter lifetime of charm hadrons, with lower decay multiplicity, and have specific features for specific hadronization and decay modes, for example $D^* \to D^0\pi$, where the soft pion tends to be aligned to the direction of the original charm quark, showing a characteristic peak at $\approx 0 p_T$ with respect to the charm jet axis. Again, the presence of two quarks of the same flavour can be exploited to measure selection efficiency from data; in addition a selection of different decay modes in the two hemispheres (e.g., a specific charm hadron exclusive decay mode on one side and the requirement of inclusive soft pion on the other side) can make two-tag correlations negligible. Here we consider for FCC-ee, an improvement

in $R_{\rm c}$ systematic precision with respect to the LEP/SLD measurements of a factor of 3, similar to the b case, leading to an uncertainty on $R_{\rm b}$ at FCC-ee of $\approx 0.15\%$. Selection of Z decays to individual light quark flavours (u, d, s) is not easy, even if low precision measurements were attempted at LEP, e.g. by selecting high momentum strange hadrons. The prerequisite for such measurements is a detailed study of fragmentation properties, with high statistics. We do not give here an estimate of possible precisions for FCC-ee, however the potential for rather precise measurements is certainly concrete.

Table 2.2 gives the statistical an systematic uncertainties on the normalized Z partial widths (R_ℓ) for various final states at FCC-ee, showing also the potential improvement with respect to LEP.

Table 2.2: Relative precision on on the normalized Z partial widths (R_ℓ) at FCC-ee. Expected statistical and systematic precisions for 150/ab are shown. The last column highligts the improvement on precision with respect to LEP.

	Statistical uncertainty	Systematic uncertainty	improvement w.r.t. LEP
R_μ (R_ℓ)	-	5×10^{-5}	20
R_τ	-	10^{-4}	20
$R_{\rm e}$	-	3×10^{-4}	20
$R_{\rm b}$	5×10^{-5}	3×10^{-4}	10
$R_{\rm c}$	1.5×10^{-4}	15×10^{-4}	10

5 The Z invisible width and the number of neutrino species

To be done after the rest *To be completed by* **Roberto** *for the standard method. To be completed by* **9th January**

Includes the standard method (recall luminosity precision) [and single photon counting. Achievable theoretical accuracy with present conceiveable technology of nu nubar gamma final states: this rather goes in the diboson section]

6 Measurement of asymmetries

Forward-backward and polarization asymmetries at the Z pole are a powerful experimental tool to investigate quarks and leptons electroweak quantum numbers and to measure the parameter regulating the difference between right-handed and left-handed couplings: the Weinberg electroweak mixing angle $\sin^2\theta_W$. With unpolarized beam, the amount of Z polarization at production is

$$\mathcal{A}_e = \frac{2g_{Ve}g_{Ae}}{(g_{Ve})^2+(g_{Ae})^2} = \frac{2g_{Ve}/g_{Ae}}{1+(g_{Ve}/g_{Ae})^2} \ . \tag{2.9}$$

The ratio of leptonic couplings is used for the operative definition of the *effective* electroweak mixing angle,

$$\sin^2\theta_{W,eff} \equiv \frac{1}{4}\left(1-\frac{g_{Ve}}{g_{Ae}}\right) \ . \tag{2.10}$$

In the parity violating decay $Z \to f\bar{f}$ the fermion is emitted preferentially in the direction of the Z with an asymmetry coefficient, for fully polarized Z, equal to $\frac{3}{4}\mathcal{A}_f$; for unpolarized beams the resulting forward backward asymmetry is $A_{FB} = \frac{3}{4}\mathcal{A}_e\mathcal{A}_f$.

In the process $e^+e^- \to Z \to f\bar{f}$, for unpolarized beams, the forward-backward asymmetry depends on both initial- and final-state couplings. For leptonic final states A_{FB} shows a quadratic dependence on the electroweak mixing angle ($\approx (1-4\sin^2\theta_{W,eff})^2$), while the dependence is essentially linear for quark final states, resulting in enhanced sensitivity to $\sin^2\theta_{W,eff}$ for quarks, in case of statistically limited measurements. At LEP A_{FB} measurements, for all final states, were limited (by far) by statistical uncertainties, therefore the most precise determination of $\sin^2\theta_{W,eff}$ was coming from b-quark final states and was made assuming the standard model structure for the b couplings. With the huge statistics expected at FCC-ee is possible to follow a different approach, i.e. use leptonic final states for a very precise determination of the electroweak mixing angle, to be used as input to quark forward-backward asymmetries for an independent determination of quark couplings.

From the experimental point of view forward backward asymmetries are robust measurements. In particular it can be shown that by exploiting differential angular distribution the measurement can be made independent of acceptance and angular corrections, provided the selection efficiency is charge- or forward-backward symmetric. The $e^+e^- \to Z \to \mu^+\mu^-$ process is a golden channel for an accurate measurement of A_{FB}; the small experimental systematic uncertainties present at LEP were related to bounds on simultaneous presence of detector and charge asymmetries, whose knowledge was limited only by data statistics, to the $\gamma\gamma \to \mu\mu$ background, which can be made negligible with appropriate cuts (and measured with data) and to the knowledge of the centre-of-mass energy, required to shift the measured asymmetry to the Z pole (m_Z). This last source of uncertainty is expected to yield the dominant systematics at FCC-ee, in spite of one order of magnitude improvement in the beam energy calibration with respect to LEP, described elsewhere in this report. The uncertainty due to this component

on $A_{FB}^{\mu\mu}$ is expected to be 2×10^{-5}, one order of magnitude larger than the expected statistical uncertainty corresponding to 150/ab, with a final uncertainty on $\sin^2\theta_{W,eff}$ of 5×10^{-6}, two order of magnitude better than the uncertainty from leptonic asymmetry obtained at LEP. Large angle Bhabha scattering $e^+e^- \to Z \to e^+e^-$ is also expected to provide information, albeit with reduced sensitivity due to the necessity of t-channel subtraction; the contribution of $e^+e^- \to Z \to \tau^+\tau^-$ is discussed later, in the context of tau polarization measurement.

The measurements of heavy quark forward-backward asymmetries can also be significantly improved at FCC-ee, as LEP results were dominated by statistical uncertainties. The $Z \to b\bar{b}$ forward-backward asymmetry can be measured with two independent techniques, one based on semileptonic b decays and the other on generic selection of b decays with lifetime tagging. The main parameters required for $A_{FB}^{b\bar{b}}$ extraction, such as the χ mixing parameter for semileptonic decays or the hemisphere charge separation for lifetime tagging, can be measured on data, utilizing the same events. The two techniques provided the same sensitivity to $A_{FB}^{b\bar{b}}$ at LEP, and the statistical uncertainty resulting from their combination was a factor of five larger than the most relevant systematic uncertainty, related to QCD corrections, giving room to significant improvements on the measurement of b couplings at FCC-ee. With a six-order of magnitude increase in the statistics of hadronic Z decays, not only the statistical uncertainty will no longer be the dominant uncertainty component, but also detector-related systematics, mostly dependent on studies based on data, will be reduced. The impact of QCD corrections will also be reduced with proper choice of analysis methods (e.g. measure the asymmetry as a function of observables sensitive to gluon radiation), taking advantage of the much higher statistics and, hopefully, with improved QCD calculations. As a simple example based on semileptonic b decays, raising the typical cut on lepton momentum from 3 GeV/c to 10 GeV/c lowers the QCD corrections to 40% of the typical LEP size with a reduction of statistics of a factor for two [**?**, **?**]. Here we conservatively assume that QCD corrections for $Z \to b\bar{b}$ (and $Z \to c\bar{c}$) asymmetries will be reduced by a factor two at FCC-ee. The conservative reduction on detector-related systematic uncertainties is assumed, yielding a total uncertainty on $A_{FB}^{b\bar{b}}$ of 30×10^{-4}, roughly a factor 5 improvement with respect to LEP.

The measurement of $A_{FB}^{c\bar{c}}$ at LEP was based on the selection of semi-exclusive charm decays (e.g. based on D^* mesons) or on semileptonic decays. The modeling of charm decays was the most seizable source of systematic uncertainties, followed by the QCD corrections. The main components of modeling where related to the lepton spectra, the multiplicity of charm decays, the effects related to the presence of $b \to c$ decays. These components are much better known already nowadays for thanks to measurements performed at b factories and will be improved in situ at FCC-ee. A conservative factor of three improvement in the knowledge of charm modeling and the factor of two already mentioned for the QCD corrections uncertainties lead to a a total uncertainty on $A_{FB}^{c\bar{c}}$ of 80×10^{-4}, a factor 4 improvement with respect to LEP.

Production of tau lepton in Z decays, $Z \to \tau^+\tau^-$, represents a special (and extremely useful) case because the polarization of the final-state fermion can be measured through the angular distributions and momenta of the decays products. The tau polarization is defined as

$$P_\tau = \frac{\sigma_R - \sigma_L}{\sigma_R + \sigma_L}, \tag{2.11}$$

its dependence on the polar angle θ can be written as

$$\mathcal{P}_\tau(\cos\theta) = \frac{A_{pol}(1+\cos^2\theta) + \frac{8}{3}A_{pol}^{FB}\cos\theta}{(1+\cos^2\theta) + \frac{8}{3}A_{FB}\cos\theta} \tag{2.12}$$

where $A_{pol} = -\mathcal{A}_\tau$, $A_{pol}^{FB} = -\frac{3}{4}\mathcal{A}_e$ and A_{FB} is as usual related to the product of initial and final state $\mathcal{A}$ factors, showing that a measurement of tau polarization as a function of θ provides a determination of both $\mathcal{A}_\tau$ and $\mathcal{A}_e$ and, consequently, a direct measurement of $\sin^2\theta_{W,eff}$. The statistical uncertainty on both $\mathcal{A}$ factors, dominating at LEP, will be negligible at FCC-ee. The main systematic uncertainties at LEP were related to the knowledge of tau branching fraction, to tau decay modeling and to higher order electroweak corrections. Improved measurements of tau branching fraction have been made at b factories and can be further improved at FCC-ee, modeling of tau decays can be similarly improved (and could be could be further reduced by using only some of the channels, by trading with statistics): here we have conservatively assumed a factor of three reduction of these uncertainties and a factor of two reduction of theory uncertainties. The resulting uncertainty on $\mathcal{A}_e$ ($\mathcal{A}_\tau$) would be 10×10^{-5} (30×10^{-5}), with an improvement of a factor of 50 (15) with respect to LEP. Note that the dependency on the beam energy is considerably reduced with respect to lepton forward-backward asymmetries, yielding a corresponding systematic uncertainty of only 10^{-5}. The measurement of $\mathcal{A}_e$ yield a determination of $\sin^2\theta_{W,eff}$ of precision similar to the one obtained from $A_{FB}^{\mu\mu}$ (6.6×10^{-6}) without assumption on electron-muon universality. The independent measurement of $\mathcal{A}_e$ can also be used to measure $\mathcal{A}_\mu$ from the muon forward-backward asymmetry.

Table 2.3 gives the statistical an systematic uncertainties on the $\mathcal{A}$ factors for the various final states expected at FCC-ee, showing the potential improvement with respect to LEP.

Table 2.3: Precision on the coupling-ratio factors $\mathcal{A}_f$ for various fermions at FCC-ee. Expected statistical and systematic precisions for 150/ab are shown. The last column highligts the improvement on precision with respect to LEP. The last two rows show the expected precision on $\sin^2\theta_{W,eff}$ from the measurement of the muon FB and tau polarization, respectively.

	Statistical uncertainty	Systematic uncertainty	improvement w.r.t. LEP
$\mathcal{A}_e$	$5. \times 10^{-5}$	$1. \times 10^{-4}$	50
$\mathcal{A}_\mu$	2.5×10^{-5}	1.5×10^{-4}	30
$\mathcal{A}_\tau$	$4. \times 10^{-5}$	$3. \times 10^{-4}$	15
$\mathcal{A}_b$	2×10^{-4}	30×10^{-4}	5
$\mathcal{A}_c$	3×10^{-4}	80×10^{-4}	4
$\sin^2\theta_{W,eff}$ (from muon FB)	10^{-7}	$5. \times 10^{-6}$	100
$\sin^2\theta_{W,eff}$ (from tau pol)	10^{-7}	6.6×10^{-6}	75

7 Extraction of fermion couplings

To be completed by **Roberto***, the precisions on A given in the table will be combined with the precisions on R_l, R_b and R_c to give the uncertainties on couplings. To be completed by* **9th January**

The couplings of the neutral current to fermions can be determined using three ingredients:

- the Z partial widths,
- the $\mathcal{A}_{\{}$ parameters as determined by the forward-backward asymmetries and tau polarization,
- the energy dependence of the forward-backward asymmetries.

The partial width of the decay $Z \to f\bar{f}$, gives the sum of the squares of the couplings, while the ratio of the vector and axial couplings is given by the leptonic measurements of $\mathcal{A}_{\{}$, i.e. by the measurement of A_{LR}, of the tau polarisation and of the leptonic forward-backward asymmetries. The energy dependence of the asymmetries fixes the value of the axial couplings, up to a common sign. This last ingredient is required, since the widths and asymmetries do not change if g_v and g_a replace each other.

8 Determination of the electromagnetic coupling constant, $\alpha_{\mathrm{QED}}(m_{\mathrm{Z}}^2)$

One page by **Patrick***, plus Fig. 6 of his paper. To be completed by* **9th January**

9 Determination of the strong coupling constant $\alpha_{\mathrm{S}}(m_{\mathrm{Z}}^2)$

Just a short overview and a pointer to the QCD section.

To be written by **Roberto***, based on the content of the QCD Section (or the Berlin talk if the QCD is not ready). To be completed by* **9th January**

10 Performance requirements for Z boson physics

10.1 Detector performance requirements

To be completed by **Roberto***, based on the input given in the past to Gigi et al.. To be completed by* **9th January**

10.2 Specific requirements on the accelerator

Just a pointer to the transverse polarization section ? Comments on the energy spread ?

To be completed by **Roberto** *by* **9th January**

Chapter 3

Di-boson physics

1 Introduction

To be done by Fulvio and Roberto after the rest

A detailed account of the di-boson physics studied at LEP is given in Ref. [3], together with the dominant sources of systematic uncertainties.

Di-boson production at FCC-ee includes $\mathrm{e^+e^-} \to \mathrm{W^+W^-}, \mathrm{ZZ}, \mathrm{Z}\gamma$ or $\gamma\gamma$ processes. The large luminosities at and above the WW threshold and up to $\sqrt{s} \sim 370$ GeV will deliver large samples of di-boson and even tri-boson events. (Give numbers.)

These large statistics enable the measurements of many electroweak parameters with unprecedented accuracies. Among these measurements are the mass and the width of the W boson, m_{W} and Γ_{W}, the trilinear and quadrilinear gauge couplings, the number of neutrino species, the strong coupling constant, or the centre-of-mass energy. The pertaining experimental strategy is outlined, and the FCC-ee potential summarized.

Give the outline of the chapter, as well as the objectives (requirements on luminosity measurement, centre-of-mass energy and energy spread measurement, detector designs, theory calculations, experimental uncertainties ...)

2 Measurement of the W mass and width at the WW threshold

The W mass is a fundamental parameter of the standard model (SM) of particle physics, currently measured with a precision of 15 MeV [4], from the combination of Tevatron and LEP2 determinations. In the context of precision electroweak precision tests the W mass direct measurement uncertainty is currently limiting the sensitivity to possible effects of new physics [5], as indirect contraints place more stringent limits of the W mass value.

A precise direct determination of the W mass can be achieved by observing the rapid rise of the W-pair production cross section near its kinematic threshold around 161 GeV. The advantages of this method are that it only involves selecting and counting events, it is clean and uses all decay channels.

W mass measurement at a single energy point

In 1996 the LEP2 collider delivered $\mathrm{e^+e^-}$ collisions at a single energy point near 161 GeV, with a total integrated luminosity of about 10 pb^{-1} at each of the four interaction points. The data was used to measure the W-pair cross section (σ_{WW}) at 161 GeV, and extract the W mass with a precision of 200 MeV [6–9].

Taking data at a single energy point the statistical sensitivity to the W mass with a simple event counting is given by

$$\Delta m_{\mathrm{W}}(\mathrm{stat}) = \left(\frac{d\sigma_{\mathrm{WW}}}{dm_{\mathrm{W}}}\right)^{-1} \frac{\sqrt{\sigma_{\mathrm{WW}}}}{\sqrt{\mathcal{L}}} \frac{1}{\sqrt{\epsilon p}} \tag{3.1}$$

where $\mathcal{L}$ is the data integrated luminosity, ϵ the event selection efficiency and p the selection purity. The purity can be also expressed as

$$p = \frac{\epsilon\sigma_{\mathrm{WW}}}{\epsilon\sigma_{\mathrm{WW}} + \sigma_B}$$

where σ_B is the total selected background cross section.

A systematic uncertainty on the background cross section will propagate to the W mass uncertainty as

$$\Delta m_{\mathrm{W}}(B) = \left(\frac{d\sigma_{\mathrm{WW}}}{dm_{\mathrm{W}}}\right)^{-1} \frac{\Delta\sigma_B}{\epsilon}. \tag{3.2}$$

Other systematic uncertainties as on the acceptance ($\Delta\epsilon$) and luminosity ($\Delta\mathcal{L}$) will propagate as

$$\Delta m_{\mathrm{W}}(\mathrm{A}) = sigma_{\mathrm{WW}} \left(\frac{d\sigma_{\mathrm{WW}}}{dm_{\mathrm{W}}}\right)^{-1} \left(\frac{\Delta\epsilon}{\epsilon} \oplus \frac{\Delta\mathcal{L}}{\mathcal{L}}\right), \tag{3.3}$$

while theoretical uncertainties on the cross section ($\Delta d\sigma_{\mathrm{WW}}$) propagate directly as

$$\Delta m_{\mathrm{W}}(\mathrm{T}) = \left(\frac{d\sigma_{\mathrm{WW}}}{dm_{\mathrm{W}}}\right)^{-1} \Delta\sigma_{\mathrm{WW}}(\mathrm{T}). \tag{3.4}$$

Finally the uncertainty on the center of mass energy E_{CM} will propagate to the W mass uncertainty as

$$\Delta m_{\mathrm{W}}(\mathrm{E}) = \left(\frac{d\sigma_{\mathrm{WW}}}{dm_{\mathrm{W}}}\right)^{-1} \left(\frac{d\sigma_{\mathrm{WW}}}{dE_{\mathrm{CM}}}\right) \Delta E_{\mathrm{CM}}, \tag{3.5}$$

that can be shown to be limited as $\Delta m_{\mathrm{W}}(\mathrm{E}) \leq \Delta E_{\mathrm{CM}}/2$, and in fact for E_{CM} near the threshold it is $\Delta m_{\mathrm{W}}(\mathrm{E}) \simeq \Delta E_{\mathrm{CM}}/2$, so it is the beam energy uncertainty that propagates directly to the W mass uncertainty.

In the case of $\mathcal{L} = 8$ ab^{-1} accumulated by the FCCee data taking in one year, and assuming the LEP event selection quality [6] with $\sigma_B = 300$ fb and $\epsilon = 0.75$, a statistical precision of $\Delta m_{\mathrm{W}} \simeq 0.35$ MeV is achievable if the systematic uncertainties will not be limiting the precision, i.e. if the following conditions are achieved:

$$\Delta\sigma_B < 0.6 \text{ fb} \tag{3.6}$$

$$\left(\frac{\Delta\epsilon}{\epsilon} \oplus \frac{\Delta\mathcal{L}}{\mathcal{L}}\right) < 2 \cdot 10^{-4} \tag{3.7}$$

$$\Delta\sigma_{\mathrm{WW}}(\mathrm{T}) < 0.8 \text{ fb} \tag{3.8}$$

$$\Delta E_{\mathrm{CM}} < 0.35 \text{ MeV} \tag{3.9}$$

corresponding to precision levels of $2 \cdot 10^{-3}$ on the background, $2 \cdot 10^{-4}$ on acceptance and luminosity, $2 \cdot 10^{-4}$ on the theoretical cross section, and $4 \cdot 10^{-6}$ on the beam energy.

W mass and width measurements at two or more energy points

In the SM the W width is well constrained by the W mass, and the Fermi constant, with a $\sim \alpha_S/\pi$ QCD correction due to the hadronic decay contributions; the W width is currently measured to a precision of 42 MeV [4]. The first calculations of the W boson width effects in $\mathrm{e^+e^-} \to \mathrm{W^+W^-}$ reactions have been performed in Ref. [10], and revealed the substantial effects

of the width on the full cross section lineshape, in particular at energies below the nominal threshold.

From the determination of σ_{WW} at a minimum of two energy points near the kinematic threshold both the W mass and width can be extracted [11].

In the following the YFSWW3 version 1.18 [12] program has been used to calculate σ_{WW} as a function of the energy (E_{CM}), W mass (m_{W}) and width (Γ_{W}). Figure 3.1 shows the W-pair cross section as a function of the $\mathrm{e^+e^-}$ collision energy with W mass and width values set at the PDG [4] average measured central values $m_{\mathrm{W}} = 80.385$ GeV and $\Gamma_{\mathrm{W}} = 2.085$ GeV, and with large 1 GeV variation bands of the mass and width central values.

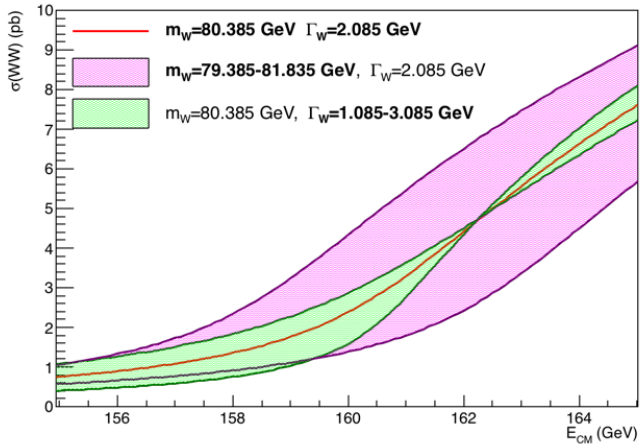

Fig. 3.1: W-pair production cross section as a function of the $\mathrm{e^+e^-}$ collision energy E_{CM} as evaluated with YFSWW3 1.18 [12]. The central curve corresponds to the predictions obtained with $m_{\mathrm{W}} = 80.385$ GeV and $\Gamma_{\mathrm{W}} = 2.085$ GeV. Purple and green bands show the cross section curves obtained varying the W mass and width by ± 1 GeV.

It can be noted that while a variation of the W mass roughly corresponds to a shift of the cross section lineshape along the energy axis, a variation of the W width has the effect of changing the slope of cross section lineshape rise. It can also be noted that the W width dependence shows a crossing point at $E_{\mathrm{CM}} \simeq 2m_{\mathrm{W}} + 1.5\mathrm{GeV} \simeq 162.3$ GeV, where the cross section is insensitive to the W width.

Figures 3.2 and 3.3 show the differential functions relevant to the statistical and systematical uncertainties for a measurement of the W mass and width from the W-pair cross section near the kinematic threshold, similarly as discussed for the single energy point W mass extraction. For the statistical terms the efficiency and purities are evaluated assuming an event selection quality with $\sigma_B \simeq 300$ fb and $\epsilon \simeq 0.75$.

The minima of the mass differential curves plotted in Fig. 3.2 indicate the optimal points to take data for a W mass measurement, in particular minimum statistical uncertainty is achieved with $E_{\mathrm{CM}} \simeq 2m_{\mathrm{W}} + 0.6$ GeV$\simeq 161.4$ GeV. The minima of the width differential curves, on Fig. 3.3, indicate maximum sensitivity to the W width, while all curves diverge at the W width insensitive point $E_{\mathrm{CM}} \simeq 162.3$ GeV, where $d\sigma_{\mathrm{WW}}/d\Gamma_{\mathrm{W}} = 0$.

If two cross section measurements $\sigma_{1,2}$ are performed at two energy points $E_{1,2}$, both the W mass and width can be extracted with a fit to the cross section lineshape. The uncertainty

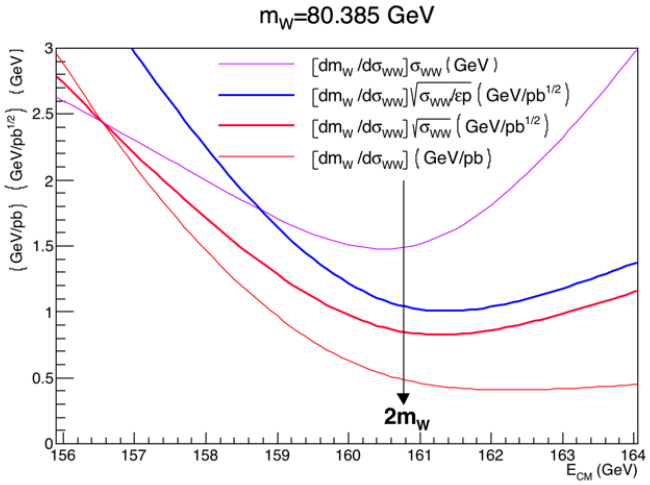

Fig. 3.2: W-pair cross section differential functions with respect to the W mass, evaluated with YFSWW3 1.18 [12]. The central mass value is set to $m_{\mathrm{W}} = 80.385$ GeV.

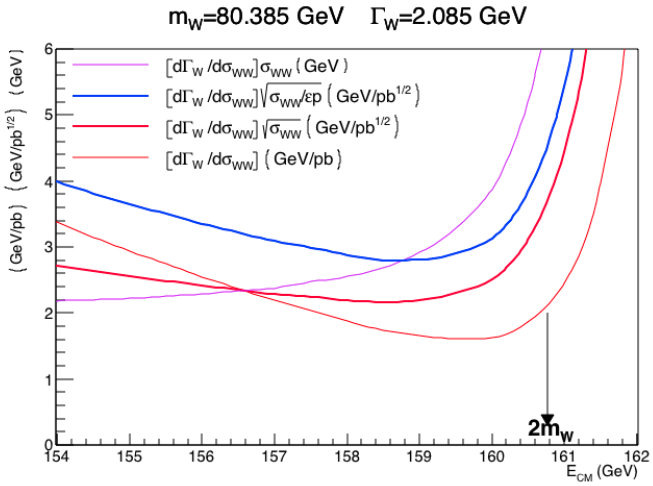

Fig. 3.3: W-pair cross section differential functions with respect to the W width, evaluated with YFSWW3 1.18 [12]. Central mass and width values are set to $m_{\mathrm{W}} = 80.385$ GeV and $\Gamma_{\mathrm{W}} = 2.085$ GeV.

propagation would then follow

$$\Delta\sigma_1 = \frac{d\sigma_1}{dm}\Delta m + \frac{d\sigma_1}{d\Gamma}\Delta\Gamma = a_1\Delta m + b_1\Delta\Gamma \tag{3.10}$$

$$\Delta\sigma_2 = \frac{d\sigma_2}{dm}\Delta m + \frac{d\sigma_2}{d\Gamma}\Delta\Gamma = a_2\Delta m + b_2\Delta\Gamma. \tag{3.11}$$

The resulting uncertainty on the W mass and width would be

$$\Delta m = -\frac{b_2\Delta\sigma_1 - b_1\Delta\sigma_2}{a_2 b_1 - a_1 b_2} \tag{3.12}$$

$$\Delta\Gamma = \frac{a_2\Delta\sigma_1 - a_1\Delta\sigma_2}{a_2 b_1 - a_1 b_2} \tag{3.13}$$

If the $\Delta\sigma_{1,2}$ uncertainties on the cross section measurements are uncorrelated, e.g. only statistical, the linear correlation between the derived mass and width uncertainties is

$$r(\Delta m, \Delta\Gamma) = \frac{1}{\Delta m \Delta\Gamma} \frac{a_2 b_2 \Delta\sigma_1^2 + a_1 b_1 \Delta\sigma_2^2}{(a_2 b_1 - a_1 b_2)^2} \tag{3.14}$$

Optimal data taking configurations

When conceiving data taking at two different energy points near the W-pair threshold in order to extract both m_{W} and Γ_{W}, it is useful to figure out which energy points values E_1 and E_2, would be optimally suited to obtain the best measurements, also as a function of the data luminosity fraction f delivered at the higher energy point. For this a full 3-dimensional scan of possible E_1 and E_2 values, with 10 MeV steps, and of f values, with 0.05 steps, has been performed, and the data taking configurations that minimize arbitrary combination of the expected statistical uncertainties on the mass and the width $F(\Delta m_{\mathrm{W}}, \Delta\Gamma_{\mathrm{W}})$ are found.

For example, in order to minimize the simple sum of the statistical uncertainties $F(\Delta m_{\mathrm{W}}, \Delta\Gamma_{\mathrm{W}}) = \Delta m_{\mathrm{W}} + \Delta\Gamma_{\mathrm{W}}$, the optimal data taking configuration would be with

$$E_1 = 157.10 \text{ GeV}, \qquad E_2 = 162.34 \text{ GeV}, \qquad f = 0.40. \tag{3.15}$$

With this configuration, and assuming a total luminosity of $\mathcal{L} = 8$ ab^{-1}, the projected statistical uncertainties would be

$$\Delta m_{\mathrm{W}} = 0.60 \text{ MeV} \qquad \text{and} \quad \Delta\Gamma_{\mathrm{W}} = 1.50 \text{ MeV}. \tag{3.16}$$

With this same data taking configuration,the statistical uncertainty obtained when measuring only the W mass would yield $\Delta m_{\mathrm{W}} = 0.55$ MeV, just slightly better with respect to the two-parameter fit. On the other hand the $\Delta m_{\mathrm{W}} = 0.55$ MeV precision obtained in this way must be compared with the $\Delta m_{\mathrm{W}} = 0.35$ MeV statistical precision obtainable when taking all data at the most optimal single energy point $E_0 = 161.4$ GeV.

When varying the $F(\Delta m_{\mathrm{W}}, \Delta\Gamma_{\mathrm{W}})$ target to optimize towards, the obtained optimal energy points don't change much, with the upper energy always at the Γ_{W}-independent $E_2 = 162.34$ GeV point, and the optimal lower E_1 point at $(1-2)\Gamma_{\mathrm{W}}$ units below the nominal $2m_{\mathrm{W}}$ threshold, $E_1 = 2m_{\mathrm{W}} - (1-2)\Gamma_{\mathrm{W}}$, according to if the desired precision is more or less focused on the W mass or the W width measurement. In a similar way the optimal data fraction to be taken at the lower off-shell E_2 energy point varies according to the chosen precision targets, with larger fractions more to the benefit of the W width precision. When a small fraction of data (e.g. f =0.05) is taken off-shell a statistical precision $\Delta m_{\mathrm{W}} = 0.39$ MeV is recovered both in the single- (m_{W}) and the two-parameter ($m_{\mathrm{W}}, \Gamma_{\mathrm{W}}$) fits.

Considering that the beam energies E_b that can surely be calibrated with resonant depolarization are such that the spin tune is a half integer, that is

$$E_b = 0.4406486(\nu + 0.5) \quad \text{GeV} \tag{3.17}$$

where ν is and integer, the scan of energy points can be limited to a grid with $E_{\mathrm{CM}} = 0.8812972(\nu + 0.5) \quad \text{GeV}$. Taking this grid constraint into account the optimal higher energy point for data taking becomes the $E_2 = 162.62$ GeV for $\nu = 184$. The corresponding optimal statistical precisions attainable are increased by 5-10% with respect to the velues reported above. For the case of minimizing $\Delta m_{\mathrm{W}} + \Delta\Gamma_{\mathrm{W}}$, would be with taking data with $E_1 = 157.33$ GeV,$E_2 = 162.62$ GeV, $f = 0.40$ and yielding statistical uncertainties $\Delta m_{\mathrm{W}} = 0.65$ MeV and $\Delta\Gamma_{\mathrm{W}} = 1.59$ MeV assuming a total integrated luminosity $\mathcal{L} = 8$ ab^{-1}.

Data taking at additional energy points

In the case of limiting correlated systematics uncertainties, it can be useful to take data and measure both signal and background cross section at more than two $E_{\rm CM}$ points, in order to reduce background and acceptance uncertainties.

In particular, for the simultaneous measurement of $m_{\rm W}$ and $\Gamma_{\rm W}$ just described, taking data at energy points where the differential factors $(d\sigma/dm_{\rm W})^{-1}$, $(d\sigma/d\Gamma_{\rm W})^{-1}$, $\sigma(d\sigma/dm_{\rm W})^{-1}$ and $\sigma(d\sigma/d\Gamma_{\rm W})^{-1}$, are equal, can help cancelling the effect of correlated systematic uncertainties of background and acceptance.

Measuring the W-pair cross section at additional points can also serve to disentagle other possible new physics effects at threshold; for example measuring the $\beta_{\rm W}^3$ raise of the triple gauge coupling (TGC) cancellation effects.

3 Measurement of W partial widths

Can be done by **Roberto** *after the rest. To be completed* **after 9th January**

Here universality tests are discussed. Also recall hadronic decays and measurement of $\alpha_{\rm S}$ (discussed in QCD chapter) and $V_{\rm cb}$.

4 Direct determinaton of the W mass and width

$$m_{12}^2 = s\frac{\beta_1 \sin\theta_1 + \beta_1 \sin\theta_1 - \beta_1\beta_2|\sin(\theta_1+\theta_2)|}{\beta_1 \sin\theta_1 + \beta_1 \sin\theta_1 - \beta_1\beta_2|\sin(\theta_1+\theta_2)|} \tag{3.18}$$

Direct determination of the W mass (and width?) from the decay product invariant mass and energy-momentum conservation is described.

The method requires the precise knowledge of the centre-of-mass energy and energy spread (?). Recall the principle, requirements, and precision from the various methods: resonant depolarization at and slightly above the WW threshold, and direct determination from ZZ and Zγ production and $m_{\rm Z}$ knowledge well above the WW threshold. Details of the method are to be given in the dedicated section. Note that the centre-of-mass energy can also be determined from WW final states with $m_{\rm W}$ knowledge (can/must be used at 240/350 GeV).

5 Cross section measurements

To be done by **Paolo**. *To be completed by* **9th January**

Describe the measurements of the WW, ZZ, Zγ cross section as a function of $\sqrt{s}$. Recall the physics case for these measurements.

6 Constraints on tri-linear and quartic gauge couplings

No reflections or activities on this part until now. The minimum is some extrapolation by **Roberto** *taking as input works done for other future machines, with help from* **Fulvio**. *To be completed* **after 9th January**

Here the measurements of TGC and QGC from ZZ, WW and single W production are discussed (angular analysis, W polarisation, effective Lagrangian).

7 Performance requirements for diboson physics

To be done by **Paolo**. *To be completed by* **9th January**

7.1 Detector performance requirements

7.2 Specific requirements on the accelerator